# Search for Neutral Supersymmetric Higgs Bosons in Multijet Events at $\sqrt{s} = 1.96$ TeV

V. M. Abazov,[35] B. Abbott,[72] M. Abolins,[63] B. S. Acharya,[29] M. Adams,[50] T. Adams,[48] M. Agelou,[18] J.-L. Agram,[19] S. H. Ahn,[31] M. Ahsan,[57] G. D. Alexeev,[35] G. Alkhazov,[39] A. Alton,[62] G. Alverson,[61] G. A. Alves,[2] M. Anastasoaie,[34] T. Andeen,[52] S. Anderson,[44] B. Andrieu,[17] Y. Arnoud,[14] A. Askew,[48] B. Åsman,[40] A. C. S. Assis Jesus,[3] O. Atramentov,[55] C. Autermann,[21] C. Avila,[8] F. Badaud,[13] A. Baden,[59] B. Baldin,[49] P. W. Balm,[33] S. Banerjee,[29] E. Barberis,[61] P. Bargassa,[76] P. Baringer,[56] C. Barnes,[42] J. Barreto,[2] J. F. Bartlett,[49] U. Bassler,[17] D. Bauer,[53] A. Bean,[56] S. Beauceron,[17] M. Begel,[68] A. Bellavance,[65] S. B. Beri,[27] G. Bernardi,[17] R. Bernhard,[49,*] I. Bertram,[41] M. Besançon,[18] R. Beuselinck,[42] V. A. Bezzubov,[38] P. C. Bhat,[49] V. Bhatnagar,[27] M. Binder,[25] C. Biscarat,[41] K. M. Black,[60] I. Blackler,[42] G. Blazey,[51] F. Blekman,[33] S. Blessing,[48] D. Bloch,[19] U. Blumenschein,[23] A. Boehnlein,[49] O. Boeriu,[54] T. A. Bolton,[57] F. Borcherding,[49] G. Borissov,[41] K. Bos,[33] T. Bose,[67] A. Brandt,[74] R. Brock,[63] G. Brooijmans,[67] A. Bross,[49] N. J. Buchanan,[48] D. Buchholz,[52] M. Buehler,[50] V. Buescher,[23] S. Burdin,[49] T. H. Burnett,[78] E. Busato,[17] C. P. Buszello,[42] J. M. Butler,[60] J. Cammin,[68] S. Caron,[33] W. Carvalho,[3] B. C. K. Casey,[73] N. M. Cason,[54] H. Castilla-Valdez,[32] S. Chakrabarti,[29] D. Chakraborty,[51] K. M. Chan,[68] A. Chandra,[29] D. Chapin,[73] F. Charles,[19] E. Cheu,[44] D. K. Cho,[60] S. Choi,[47] B. Choudhary,[28] T. Christiansen,[25] L. Christofek,[56] D. Claes,[65] B. Clément,[19] C. Clément,[40] Y. Coadou,[5] M. Cooke,[76] W. E. Cooper,[49] D. Coppage,[56] M. Corcoran,[76] A. Cothenet,[15] M.-C. Cousinou,[15] B. Cox,[43] S. Crépé-Renaudin,[14] D. Cutts,[73] H. da Motta,[2] B. Davies,[41] G. Davies,[42] G. A. Davis,[52] K. De,[74] P. de Jong,[33] S. J. de Jong,[34] E. De La Cruz-Burelo,[32] C. De Oliveira Martins,[3] S. Dean,[43] J. D. Degenhardt,[62] F. Déliot,[18] M. Demarteau,[49] R. Demina,[68] P. Demine,[18] D. Denisov,[49] S. P. Denisov,[38] S. Desai,[69] H. T. Diehl,[49] M. Diesburg,[49] M. Doidge,[41] H. Dong,[69] S. Doulas,[61] L. V. Dudko,[37] L. Duflot,[16] S. R. Dugad,[29] A. Duperrin,[15] J. Dyer,[63] A. Dyshkant,[51] M. Eads,[51] D. Edmunds,[63] T. Edwards,[43] J. Ellison,[47] J. Elmsheuser,[25] V. D. Elvira,[49] S. Eno,[59] P. Ermolov,[37] O. V. Eroshin,[38] J. Estrada,[49] H. Evans,[67] A. Evdokimov,[36] V. N. Evdokimov,[38] J. Fast,[49] S. N. Fatakia,[60] L. Feligioni,[60] A. V. Ferapontov,[38] T. Ferbel,[68] F. Fiedler,[25] F. Filthaut,[34] W. Fisher,[66] H. E. Fisk,[49] I. Fleck,[23] M. Fortner,[51] H. Fox,[23] S. Fu,[49] S. Fuess,[49] T. Gadfort,[78] C. F. Galea,[34] E. Gallas,[49] E. Galyaev,[54] C. Garcia,[68] A. Garcia-Bellido,[78] J. Gardner,[56] V. Gavrilov,[36] P. Gay,[13] D. Gelé,[19] R. Gelhaus,[47] K. Genser,[49] C. E. Gerber,[50] Y. Gershtein,[48] D. Gillberg,[5] G. Ginther,[68] T. Golling,[22] N. Gollub,[40] B. Gómez,[8] K. Gounder,[49] A. Goussiou,[54] P. D. Grannis,[69] S. Greder,[3] H. Greenlee,[49] Z. D. Greenwood,[58] E. M. Gregores,[4] Ph. Gris,[13] J.-F. Grivaz,[16] L. Groer,[67] S. Grünendahl,[49] M. W. Grünewald,[30] S. N. Gurzhiev,[38] G. Gutierrez,[49] P. Gutierrez,[72] A. Haas,[67] N. J. Hadley,[59] S. Hagopian,[48] I. Hall,[72] R. E. Hall,[46] C. Han,[62] L. Han,[7] K. Hanagaki,[49] K. Harder,[57] A. Harel,[26] R. Harrington,[61] J. M. Hauptman,[55] R. Hauser,[63] J. Hays,[52] T. Hebbeker,[21] D. Hedin,[51] J. M. Heinmiller,[50] A. P. Heinson,[47] U. Heintz,[60] C. Hensel,[56] G. Hesketh,[61] M. D. Hildreth,[54] R. Hirosky,[77] J. D. Hobbs,[69] B. Hoeneisen,[12] M. Hohlfeld,[24] S. J. Hong,[31] R. Hooper,[73] P. Houben,[33] Y. Hu,[69] J. Huang,[53] V. Hynek,[9] I. Iashvili,[47] R. Illingworth,[49] A. S. Ito,[49] S. Jabeen,[56] M. Jaffré,[16] S. Jain,[72] V. Jain,[70] K. Jakobs,[23] A. Jenkins,[42] R. Jesik,[42] K. Johns,[44] M. Johnson,[49] A. Jonckheere,[49] P. Jonsson,[42] A. Juste,[49] D. Käfer,[21] S. Kahn,[70] E. Kajfasz,[15] A. M. Kalinin,[35] J. Kalk,[63] D. Karmanov,[37] J. Kasper,[60] D. Kau,[48] R. Kaur,[27] R. Kehoe,[75] S. Kermiche,[15] S. Kesisoglou,[73] A. Khanov,[68] A. Kharchilava,[54] Y. M. Kharzheev,[35] H. Kim,[74] T. J. Kim,[31] B. Klima,[49] J. M. Kohli,[27] M. Kopal,[72] V. M. Korablev,[38] J. Kotcher,[70] B. Kothari,[67] A. Koubarovsky,[37] A. V. Kozelov,[38] J. Kozminski,[63] A. Kryemadhi,[77] S. Krzywdzinski,[49] Y. Kulik,[49] A. Kumar,[28] S. Kunori,[59] A. Kupco,[11] T. Kurča,[20] J. Kvita,[9] S. Lager,[40] N. Lahrichi,[18] G. Landsberg,[73] J. Lazoflores,[48] A.-C. Le Bihan,[19] P. Lebrun,[20] W. M. Lee,[48] A. Leflat,[37] F. Lehner,[49,*] C. Leonidopoulos,[67] J. Leveque,[44] P. Lewis,[42] J. Li,[74] Q. Z. Li,[49] J. G. R. Lima,[51] D. Lincoln,[49] S. L. Linn,[48] J. Linnemann,[63] V. V. Lipaev,[38] R. Lipton,[49] L. Lobo,[42] A. Lobodenko,[39] M. Lokajicek,[11] A. Lounis,[19] P. Love,[41] H. J. Lubatti,[78] L. Lueking,[49] M. Lynker,[54] A. L. Lyon,[49] A. K. A. Maciel,[51] R. J. Madaras,[45] P. Mättig,[26] C. Magass,[21] A. Magerkurth,[62] A.-M. Magnan,[14] N. Makovec,[16] P. K. Mal,[29] H. B. Malbouisson,[3] S. Malik,[58] V. L. Malyshev,[35] H. S. Mao,[6] Y. Maravin,[49] M. Martens,[49] S. E. K. Mattingly,[73] A. A. Mayorov,[38] R. McCarthy,[69] R. McCroskey,[44] D. Meder,[24] A. Melnitchouk,[64] A. Mendes,[15] M. Merkin,[37] K. W. Merritt,[49] A. Meyer,[21] J. Meyer,[22] M. Michaut,[18] H. Miettinen,[76] J. Mitrevski,[67] J. Molina,[3] N. K. Mondal,[29] R. W. Moore,[5] G. S. Muanza,[20] M. Mulders,[49] Y. D. Mutaf,[69] E. Nagy,[15] M. Narain,[60] N. A. Naumann,[34] H. A. Neal,[62] J. P. Negret,[8] S. Nelson,[48] P. Neustroev,[39] C. Noeding,[23] A. Nomerotski,[49] S. F. Novaes,[4] T. Nunnemann,[25] E. Nurse,[43] V. O'Dell,[49] D. C. O'Neil,[5] V. Oguri,[3] N. Oliveira,[3] N. Oshima,[49] G. J. Otero y Garzón,[50] P. Padley,[76] N. Parashar,[58] S. K. Park,[31] J. Parsons,[67] R. Partridge,[73] N. Parua,[69] A. Patwa,[70] G. Pawloski,[76] P. M. Perea,[47] E. Perez,[18] P. Pétroff,[16] M. Petteni,[42] R. Piegaia,[1] M.-A. Pleier,[68] P. L. M. Podesta-Lerma,[32] V. M. Podstavkov,[49] Y. Pogorelov,[54] A. Pompoš,[72] B. G. Pope,[63] W. L. Prado da Silva,[3]

 

H. B. Prosper,[48] S. Protopopescu,[70] J. Qian,[62] A. Quadt,[22] B. Quinn,[64] K. J. Rani,[29] K. Ranjan,[28] P. A. Rapidis,[49] P. N. Ratoff,[41] S. Reucroft,[61] M. Rijssenbeek,[69] I. Ripp-Baudot,[19] F. Rizatdinova,[57] S. Robinson,[42] R. F. Rodrigues,[3] C. Royon,[18] P. Rubinov,[49] R. Ruchti,[54] V. I. Rud,[37] G. Sajot,[14] A. Sánchez-Hernández,[32] M. P. Sanders,[59] A. Santoro,[3] G. Savage,[49] L. Sawyer,[58] T. Scanlon,[42] D. Schaile,[25] R. D. Schamberger,[69] H. Schellman,[52] P. Schieferdecker,[25] C. Schmitt,[26] C. Schwanenberger,[22] A. Schwartzman,[66] R. Schwienhorst,[63] S. Sengupta,[48] H. Severini,[72] E. Shabalina,[50] M. Shamim,[57] V. Shary,[18] A. A. Shchukin,[38] W. D. Shephard,[54] R. K. Shivpuri,[28] D. Shpakov,[61] R. A. Sidwell,[57] V. Simak,[10] V. Sirotenko,[49] P. Skubic,[72] P. Slattery,[68] R. P. Smith,[49] K. Smolek,[10] G. R. Snow,[65] J. Snow,[71] S. Snyder,[70] S. Söldner-Rembold,[43] X. Song,[51] L. Sonnenschein,[17] A. Sopczak,[41] M. Sosebee,[74] K. Soustruznik,[9] M. Souza,[2] B. Spurlock,[74] N. R. Stanton,[57] J. Stark,[14] J. Steele,[58] K. Stevenson,[53] V. Stolin,[36] A. Stone,[50] D. A. Stoyanova,[38] J. Strandberg,[40] M. A. Strang,[74] M. Strauss,[72] R. Ströhmer,[25] D. Strom,[52] M. Strovink,[45] L. Stutte,[49] S. Sumowidagdo,[48] A. Sznajder,[3] M. Talby,[15] P. Tamburello,[44] W. Taylor,[5] P. Telford,[43] J. Temple,[44] M. Tomoto,[49] T. Toole,[59] J. Torborg,[54] S. Towers,[69] T. Trefzger,[24] S. Trincaz-Duvoid,[17] B. Tuchming,[18] C. Tully,[66] A. S. Turcot,[43] P. M. Tuts,[67] L. Uvarov,[39] S. Uvarov,[39] S. Uzunyan,[51] B. Vachon,[5] R. Van Kooten,[53] W. M. van Leeuwen,[33] N. Varelas,[50] E. W. Varnes,[44] A. Vartapetian,[74] I. A. Vasilyev,[38] M. Vaupel,[26] P. Verdier,[20] L. S. Vertogradov,[35] M. Verzocchi,[59] F. Villeneuve-Seguier,[42] J.-R. Vlimant,[17] E. Von Toerne,[57] M. Vreeswijk,[33] T. Vu Anh,[16] H. D. Wahl,[48] L. Wang,[59] J. Warchol,[54] G. Watts,[78] M. Wayne,[54] M. Weber,[49] H. Weerts,[63] M. Wegner,[21] N. Wermes,[22] A. White,[74] V. White,[49] D. Wicke,[49] D. A. Wijngaarden,[34] G. W. Wilson,[56] S. J. Wimpenny,[47] J. Wittlin,[60] M. Wobisch,[49] J. Womersley,[49] D. R. Wood,[61] T. R. Wyatt,[43] Q. Xu,[62] N. Xuan,[54] S. Yacoob,[52] R. Yamada,[49] M. Yan,[59] T. Yasuda,[49] Y. A. Yatsunenko,[35] Y. Yen,[26] K. Yip,[70] H. D. Yoo,[73] S. W. Youn,[52] J. Yu,[74] A. Yurkewicz,[69] A. Zabi,[16] A. Zatserklyaniy,[51] M. Zdrazil,[69] C. Zeitnitz,[24] D. Zhang,[49] X. Zhang,[72] T. Zhao,[78] Z. Zhao,[62] B. Zhou,[62] J. Zhu,[69] M. Zielinski,[68] D. Zieminska,[53] A. Zieminski,[53] R. Zitoun,[69] V. Zutshi,[51] and E. G. Zverev[37]

(D0 Collaboration)

[1]*Universidad de Buenos Aires, Buenos Aires, Argentina*
[2]*LAFEX, Centro Brasileiro de Pesquisas Físicas, Rio de Janeiro, Brazil*
[3]*Universidade do Estado do Rio de Janeiro, Rio de Janeiro, Brazil*
[4]*Instituto de Física Teórica, Universidade Estadual Paulista, São Paulo, Brazil*
[5]*University of Alberta, Edmonton, Alberta, Canada, Simon Fraser University, Burnaby, British Columbia, Canada, York University, Toronto, Ontario, Canada, and McGill University, Montreal, Quebec, Canada*
[6]*Institute of High Energy Physics, Beijing, People's Republic of China*
[7]*University of Science and Technology of China, Hefei, People's Republic of China*
[8]*Universidad de los Andes, Bogotá, Colombia*
[9]*Center for Particle Physics, Charles University, Prague, Czech Republic*
[10]*Czech Technical University, Prague, Czech Republic*
[11]*Institute of Physics, Academy of Sciences, Center for Particle Physics, Prague, Czech Republic*
[12]*Universidad San Francisco de Quito, Quito, Ecuador*
[13]*Laboratoire de Physique Corpusculaire, IN2P3-CNRS, Université Blaise Pascal, Clermont-Ferrand, France*
[14]*Laboratoire de Physique Subatomique et de Cosmologie, IN2P3-CNRS, Universite de Grenoble 1, Grenoble, France*
[15]*CPPM, IN2P3-CNRS, Université de la Méditerranée, Marseille, France*
[16]*Laboratoire de l'Accélérateur Linéaire, IN2P3-CNRS, Orsay, France*
[17]*LPNHE, IN2P3-CNRS, Universités Paris VI and VII, Paris, France*
[18]*DAPNIA/Service de Physique des Particules, CEA, Saclay, France*
[19]*IReS, IN2P3-CNRS, Université Louis Pasteur, Strasbourg, France, and Université de Haute Alsace, Mulhouse, France*
[20]*Institut de Physique Nucléaire de Lyon, IN2P3-CNRS, Université Claude Bernard, Villeurbanne, France*
[21]*III. Physikalisches Institut A, RWTH Aachen, Aachen, Germany*
[22]*Physikalisches Institut, Universität Bonn, Bonn, Germany*
[23]*Physikalisches Institut, Universität Freiburg, Freiburg, Germany*
[24]*Institut für Physik, Universität Mainz, Mainz, Germany*
[25]*Ludwig-Maximilians-Universität München, München, Germany*
[26]*Fachbereich Physik, University of Wuppertal, Wuppertal, Germany*
[27]*Panjab University, Chandigarh, India*
[28]*Delhi University, Delhi, India*
[29]*Tata Institute of Fundamental Research, Mumbai, India*
[30]*University College Dublin, Dublin, Ireland*
[31]*Korea Detector Laboratory, Korea University, Seoul, Korea*

[32]CINVESTAV, Mexico City, Mexico
[33]FOM-Institute NIKHEF and University of Amsterdam/NIKHEF, Amsterdam, The Netherlands
[34]Radboud University Nijmegen/NIKHEF, Nijmegen, The Netherlands
[35]Joint Institute for Nuclear Research, Dubna, Russia
[36]Institute for Theoretical and Experimental Physics, Moscow, Russia
[37]Moscow State University, Moscow, Russia
[38]Institute for High Energy Physics, Protvino, Russia
[39]Petersburg Nuclear Physics Institute, St. Petersburg, Russia
[40]Lund University, Lund, Sweden, Royal Institute of Technology and Stockholm University, Stockholm, Sweden, and Uppsala University, Uppsala, Sweden
[41]Lancaster University, Lancaster, United Kingdom
[42]Imperial College, London, United Kingdom
[43]University of Manchester, Manchester, United Kingdom
[44]University of Arizona, Tucson, Arizona 85721, USA
[45]Lawrence Berkeley National Laboratory and University of California, Berkeley, California 94720, USA
[46]California State University, Fresno, California 93740, USA
[47]University of California, Riverside, California 92521, USA
[48]Florida State University, Tallahassee, Florida 32306, USA
[49]Fermi National Accelerator Laboratory, Batavia, Illinois 60510, USA
[50]University of Illinois at Chicago, Chicago, Illinois 60607, USA
[51]Northern Illinois University, DeKalb, Illinois 60115, USA
[52]Northwestern University, Evanston, Illinois 60208, USA
[53]Indiana University, Bloomington, Indiana 47405, USA
[54]University of Notre Dame, Notre Dame, Indiana 46556, USA
[55]Iowa State University, Ames, Iowa 50011, USA
[56]University of Kansas, Lawrence, Kansas 66045, USA
[57]Kansas State University, Manhattan, Kansas 66506, USA
[58]Louisiana Tech University, Ruston, Louisiana 71272, USA
[59]University of Maryland, College Park, Maryland 20742, USA
[60]Boston University, Boston, Massachusetts 02215, USA
[61]Northeastern University, Boston, Massachusetts 02115, USA
[62]University of Michigan, Ann Arbor, Michigan 48109, USA
[63]Michigan State University, East Lansing, Michigan 48824, USA
[64]University of Mississippi, University, Mississippi 38677, USA
[65]University of Nebraska, Lincoln, Nebraska 68588, USA
[66]Princeton University, Princeton, New Jersey 08544, USA
[67]Columbia University, New York, New York 10027, USA
[68]University of Rochester, Rochester, New York 14627, USA
[69]State University of New York, Stony Brook, New York 11794, USA
[70]Brookhaven National Laboratory, Upton, New York 11973, USA
[71]Langston University, Langston, Oklahoma 73050, USA
[72]University of Oklahoma, Norman, Oklahoma 73019, USA
[73]Brown University, Providence, Rhode Island 02912, USA
[74]University of Texas, Arlington, Texas 76019, USA
[75]Southern Methodist University, Dallas, Texas 75275, USA
[76]Rice University, Houston, Texas 77005, USA
[77]University of Virginia, Charlottesville, Virginia 22901, USA
[78]University of Washington, Seattle, Washington 98195, USA

(Received 11 April 2005; published 4 October 2005)

We have performed a search for neutral Higgs bosons produced in association with bottom quarks in $p\bar{p}$ collisions, using 260 $\mathrm{pb}^{-1}$ of data collected with the D0 detector in Run II of the Fermilab Tevatron Collider. The cross sections for these processes are enhanced in many extensions of the standard model (SM), such as in its minimal supersymmetric extension at large $\tan\beta$. The results of our analysis agree with expectations from the SM, and we use our measurements to set upper limits on the production of neutral Higgs bosons in the mass range of 90 to 150 GeV.

DOI: 10.1103/PhysRevLett.95.151801 PACS numbers: 14.80.Cp, 12.38.Qk, 12.60.Fr, 13.85.Rm

In two-Higgs-doublet models of electroweak symmetry breaking, such as the minimal supersymmetric extension of the standard model (MSSM) [1], there are five physical Higgs bosons: two neutral $CP$-even scalars, $h$ and $H$, with

$H$ being the heavier state; a neutral $CP$-odd state, $A$; and two charged states, $H^{\pm}$. The ratio of the vacuum expectation values of the two Higgs fields is defined as $\tan\beta = v_u/v_d$, where $v_u$ and $v_d$ refer to the fields that couple to the up-type and down-type fermions, respectively. At tree level, the coupling of the $A$ boson to down-type quarks, such as the $b$ quark, is enhanced by a factor of $\tan\beta$ relative to the standard model (SM), and the production cross section is therefore enhanced by $\tan^2\beta$ [2]. At large $\tan\beta$, this is also true either for the $h$ or $H$ bosons depending on their mass.

For several representative scenarios of the MSSM, LEP experiments have excluded at the 95% C.L. a light Higgs boson with mass $m_h < 92.9$ GeV [3]. At hadron colliders, neutral Higgs bosons can be produced in association with $b$ quarks, leading to final states containing three or four $b$ jets. The CDF experiment at the Tevatron Collider performed a search for these events in data from Run I [4]. Although their analysis was excluding some large values of $\tan\beta$ for $m_A$ up to 250 GeV, the parton distribution functions (PDFs) used to simulate the signal have been superseded. The resulting limits with the most recent PDFs would be much less stringent, hence we do not compare our current results to those from Run I.

Higgs boson production in association with $b$ quarks in $p\bar{p}$ collisions can be calculated in two ways: in the five-flavor scheme [5], only one $b$ quark has to be present, while in the four-flavor scheme [6], two $b$ quarks are explicitly required in the final state. Both calculations are now available at next-to-leading order (NLO), and agree within their respective theoretical uncertainties [7,8]. Figure 1 illustrates these processes for $h$ production at leading order (LO), and analogous diagrams can be drawn for the $H$ and $A$ bosons.

In this Letter, we assume $CP$ conservation in the Higgs sector. The masses, widths, and branching fractions for the neutral Higgs bosons into $b\bar{b}$ pairs are calculated using the CPSUPERH program [9,10]. The current analysis is sensitive

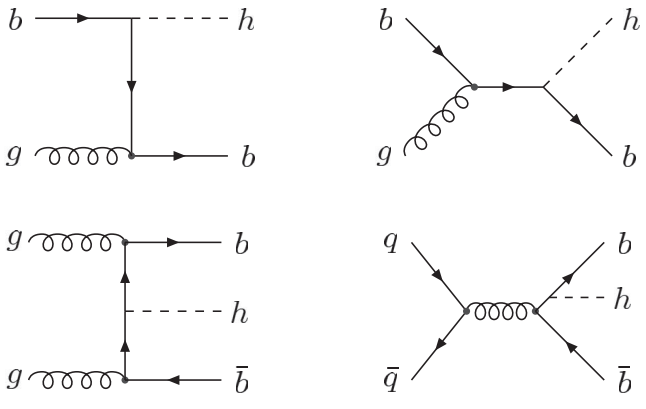


FIG. 1. Leading-order Feynman diagrams for neutral Higgs boson production in the five-flavor scheme (top) and four-flavor scheme (bottom).

to $\tan\beta$ in the range 50–100, and depends on the Higgs boson mass. In this region of $\tan\beta$, the $A$ boson is nearly degenerate in mass with either the $h$ or the $H$ boson, and their widths are small compared to the di-jet mass resolution. Consequently, we cannot distinguish between the $h/H$ and the $A$, and the total cross section for signal is assumed to be twice that of the $A$ boson. In the region of $m_A$ from 100 to 130 GeV, all three neutral Higgs bosons can be degenerate in mass and produced simultaneously [11]. Nevertheless, the total cross section still remains twice that of the $A$ boson. Using data collected by the D0 detector from November 2002 to June 2004, corresponding to an integrated luminosity of about 260 pb$^{-1}$, we search for an excess in the invariant mass distribution of the two leading transverse momentum ($p_T$) jets in events containing three or more $b$ quark candidates.

The D0 detector has a magnetic central tracking system surrounded by a uranium/liquid-argon calorimeter, contained within a muon spectrometer. The tracking system consists of a silicon microstrip tracker (SMT) and a central fiber tracker (CFT), both located within a 2 T solenoidal magnet [12]. The SMT and CFT have designs optimized for tracking and vertexing at pseudorapidities $|\eta| < 2.5$, where $\eta = -\ln[\tan(\theta/2)]$ and $\theta$ is the polar angle with respect to the proton beam direction ($z$). The calorimeter has a central section (CC) covering up to $|\eta| \approx 1.1$, and two end calorimeters (EC) extending coverage to $|\eta| \approx 4.2$, all housed in separate cryostats [13]. The calorimeter is divided into an electromagnetic part followed by fine and coarse hadronic sections. Scintillators between the CC and EC cryostats provide additional sampling of developing showers for $1.1 < |\eta| < 1.4$. The muon system consists of a layer of tracking detectors and scintillation trigger counters in front of 1.8 T toroidal magnets, followed by two similar layers behind the toroids, which provide muon tracking for $|\eta| < 2$. The luminosity is measured using scintillator arrays located in front of the EC cryostats, covering $2.7 < |\eta| < 4.4$. The trigger system comprises three levels ($L1$, $L2$, and $L3$), each performing an increasingly detailed event reconstruction in order to select the events of interest.

The large cross section for multijet production necessitates a specialized trigger to maximize signal acceptance while providing reasonable rates. This trigger at $L1$ requires signals in at least three calorimeter towers of size $\Delta\eta \times \Delta\varphi = 0.2 \times 0.2$ (where $\varphi$ is the azimuthal angle), each with transverse energy $E_T > 5$ GeV; three clusters and $H_T^{L2} > 50$ GeV at $L2$ ($H_T^{L2} \equiv$ scalar sum of the $L2$ clusters $E_T$ with $E_T > 5$ GeV), and three jets with $p_T > 15$ GeV at $L3$. A total of $87 \times 10^6$ events were selected offline with one jet of $p_T > 20$ GeV and at least two more jets with $p_T > 15$ GeV. Jets are reconstructed using a Run II cone algorithm [14] with radius $\Delta\mathcal{R} = \sqrt{(\Delta\eta)^2 + (\Delta\varphi)^2} < 0.5$, and are then required to pass a set of quality criteria. To be accepted for further analysis,

jets with $p_T > 15$ GeV must have $|\eta| < 2.5$. The jet energies are corrected to the particle level using $\eta$-dependent scale factors. Events with up to five jets are selected if they have a primary vertex position $|z| < 35$ cm and at least three jets with corrected $p_T > 35$, 20, and 15 GeV. The final selections are chosen to optimize the expected signal significance, defined as $S/\sqrt{B}$, where $S(B)$ refers to the number of signal (background) events. The window size used for optimization is Higgs boson mass dependent, taken to be $\pm 1.5$ s.d. of the signal peak, and varies from 24 to 36 GeV, for masses from 90 to 150 GeV. Jets containing $b$ quarks are identified using a secondary vertex (SV) tagging algorithm. A jet is tagged as a $b$ jet if it has at least one SV within $\Delta\mathcal{R} < 0.5$ of the jet axis and a transverse displacement from the primary vertex that exceeds 5 times the displacement uncertainty. Jets are $b$ tagged up to $|\eta| < 2.5$, although the $b$ tagging is about twice as efficient in the central region ($|\eta| < 1.1$) because of the CFT coverage. The $b$ tagging efficiency is $\approx 55\%$ for central $b$ jets of $p_T > 35$ GeV, with a light-quark (or gluon) tag rate of about 1%.

Signal events were simulated using the PYTHIA [15] event generator followed by the full D0 detector simulation and reconstruction chain. PYTHIA minimum-bias events were added to all generated events, using a Poisson probability with a mean of 0.4 events to match the instantaneous luminosities at which the data were taken [$(1–6) \times 10^{31}$ cm$^{-2}$ s$^{-1}$]. The $bh$ events, with $g \to b\bar{b}$, were generated for Higgs boson masses from 90 to 150 GeV. Reconstructed jets in simulated events were corrected to match the jet reconstruction and identification efficiencies in data. The energy of simulated jets was smeared to match the measured jet energy resolution. The $p_T$ and rapidity spectra of the Higgs bosons from PYTHIA were compared to those from the NLO calculation [5]. The shapes were similar, indicating that the PYTHIA kinematics are approximately correct. The simulated events were weighted to match the $p_T$ spectrum of the Higgs boson given by NLO, resulting in a 10% reduction of the overall signal efficiency.

Of all SM processes, multijet production is the major source of background. This background is determined from data by normalizing distributions outside of the signal region. As a cross-check, we also compare data with simulations. ALPGEN [16] is used to generate three samples of events for $b\bar{b}j$ and $b\bar{b}jj$ with $j$ corresponding to up, down, strange or charm quarks, or gluons, and $b\bar{b}b\bar{b}$ final states with generator-level requirements: $p_T^b > 25$ GeV, $p_T^j > 15$ GeV, $|\eta| < 3.0$, and $\Delta\mathcal{R} > 0.4$ between any two final-state partons. These selections do not introduce significant bias because the final sample contains much harder jets, after the application of trigger and $b$-tagging requirements. Samples of $b\bar{b}j$ and $b\bar{b}jj$ are added together, but the $b\bar{b}jj$ sample is weighted by 0.85 to match the jet multiplicity observed in doubly $b$-tagged data. The cross sections obtained from ALPGEN are 8.9 nb, 3.9 nb, and 60 pb, for the respective three states. All other backgrounds are expected to be small and are simulated with PYTHIA: $p\bar{p} \to Z(\to b\bar{b}) +$ jets, $p\bar{p} \to Zb$, and $p\bar{p} \to t\bar{t}$. Cross sections of 1.2 nb, 40 pb [17], and 7 pb are assumed, respectively.

There are two main categories of multijet background. One contains genuine heavy-flavor (HF) jets, while the other has only light-quark or gluon jets that are mistakenly tagged as $b$-quark jets, or correspond to gluons that branch into nearly collinear $b\bar{b}$ pairs. Using the selected data sample, before the application of $b$-tagging requirements, the probability to $b$ tag a jet is measured as a function of its $p_T$ in three $|\eta|$ regions. These functions are called "mistag" functions. They are corrected for the contamination from true HF events by subtracting the estimated fraction of $b\bar{b}j(j)$ events in the multijet data sample (1.2%), obtained from an initial fit to the doubly $b$-tagged data. These corrected mistag functions are then used to estimate the mistagged background by applying them to every jet reconstructed in the full data sample.

In order to test the modeling of the mistag background, the high statistics doubly $b$-tagged data are compared to simulations first, before extrapolating to the triply $b$-tagged background. The expected signal contribution to the doubly $b$-tagged data is negligible. The comparison in invariant mass spectrum of the two jets of highest $p_T$ (not necessarily the two $b$-tagged jets) in the doubly $b$-tagged data with the expected background is shown in Fig. 2. The $b$ tagging in this analysis does not distinguish between contributions from bottom and charm events. However, the efficiency for tagging a $c$ jet is known from simulations to be about $1/4$ of that for tagging a $b$ jet. Therefore, when two $b$ tags are required, the fraction of $c\bar{c}j(j)$ events relative to $b\bar{b}j(j)$ events will be a factor of $\approx 16$ lower

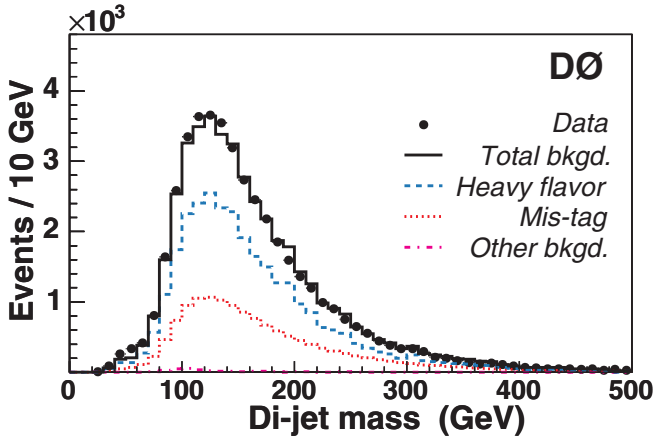


FIG. 2 (color online). Fit of the invariant mass spectrum of the two leading $p_T$ jets in the doubly $b$-tagged data to a sum of backgrounds: mistags derived from data (dotted line), $b\bar{b}j(j)$ (dashed line), and other backgrounds ($Z(\to b\bar{b}) +$ jets, $Zb$, $t\bar{t}$, and $b\bar{b}b\bar{b}$) (dash-dotted line).

TABLE I. Signal acceptances for each set of criteria (in %).

| $m_A$ (GeV) | Trigger | Kinematic | $b$ Tag | Total |
|---|---|---|---|---|
| 90 | 44 | 18 | 3.5 | 0.3 |
| 100 | 45 | 24 | 3.5 | 0.4 |
| 110 | 56 | 24 | 3.9 | 0.5 |
| 120 | 60 | 27 | 4.2 | 0.7 |
| 130 | 65 | 29 | 4.3 | 0.8 |
| 150 | 76 | 31 | 4.4 | 1.0 |

after tagging. We have estimated the fractions of $c\bar{c}jj$ to $b\bar{b}jj$ prior to $b$ tagging using the MADGRAPH Monte Carlo generator [18]. The $c\bar{c}jj$ cross section is 22% higher than $b\bar{b}jj$ for the same generator-level selections. Therefore, the contribution of $c\bar{c}j(j)$ in the doubly $b$-tagged data sample is expected to represent about 8% of the events. Thus, when we refer to the $b\bar{b}j(j)$ normalization, it should be understood that approximately 8% of the events are from the $c\bar{c}j(j)$ process. After these corrections for $c\bar{c}j(j)$ events, the HF multijet processes are only a factor of 1.08 higher in data than predicted by ALPGEN. The shape of the estimated background agrees well with the data over the entire invariant mass region.

To estimate the background for triply $b$-tagged events, the mistag function is applied to the non-$b$-tagged jets in the doubly $b$-tagged events. This provides the shape of the multijet background distribution with at least three $b$-tagged jets. This neglects any contributions from processes with more than two true $b$ jets, such as from $b\bar{b}b\bar{b}$ and $Z(\rightarrow b\bar{b})b\bar{b}$ production. However, the shapes of these backgrounds from simulations are similar to those of the doubly $b$-tagged spectra, and their rates are small. The overall background normalization is therefore determined by fitting the leading two jets invariant mass spectrum in triply $b$-tagged events outside of the hypothesized signal region to the estimated shape for triply $b$-tagged background. The systematic effect on the normalization of the background from any signal contributing outside the search window was studied and found to be small relative to other uncertainties, as described below.

The selections in this analysis can be grouped into trigger level, kinematic ($p_T$, $\eta$, $\eta_j$), where $n_j$ is the number of untagged jets, and $b$ tagging. Table I shows the acceptances for each set of criteria made in the analysis, for six values of Higgs boson mass. The systematic uncertainty on signal acceptance is nearly independent of assumed $m_A$, and is dominated by the uncertainty on $b$-tagging efficiency ( $\pm$ 15%), followed by uncertainties on jet energy scale, resolution, and identification efficiency ( $\pm$ 9% in sum). These uncertainties are calculated by repeating the analysis with each value changed by $\pm$ 1 standard deviation (s.d.). The systematic uncertainties corresponding to uncertainties in $p_T$ distributions for simulated signal at NLO, the integrated luminosity, and the trigger efficiency

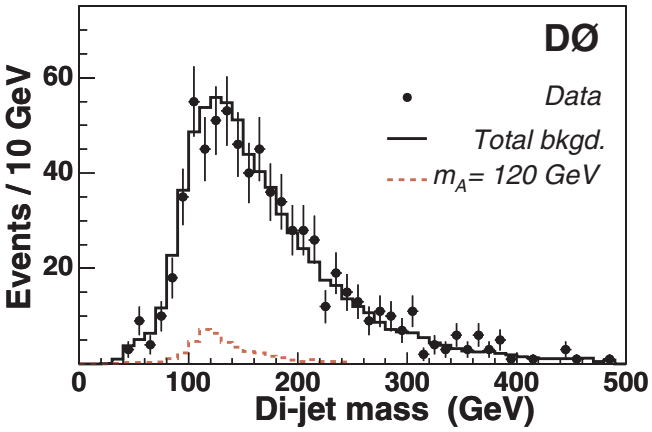


FIG. 3 (color online). Invariant mass spectrum of two leading jets in events with at least three $b$-tagged jets, estimated background, and the signal for a 120 GeV Higgs boson that can be excluded at the 95% C.L.

are found to be $\pm$5%, $\pm$6.5%, and $\pm$9%, respectively. These uncertainties, added in quadrature, result in a total systematic uncertainty of $\pm$21%.

The accuracy in modeling the shape of the background distribution can be estimated from the $\chi^2/\mathrm{dof}$ between the estimated background and the data. The statistical error associated with the uncertainty in the normalization of the background (from the fit outside the signal region) is multiplied by $\sqrt{\chi^2/\mathrm{dof}}$. The background uncertainty is estimated to be $\lesssim 3\%$. The systematic uncertainty arising from the width chosen for the search window is evaluated by varying it from $\pm$1 to $\pm$2 s.d., centered on the peak value. The resulting change in background normalization is

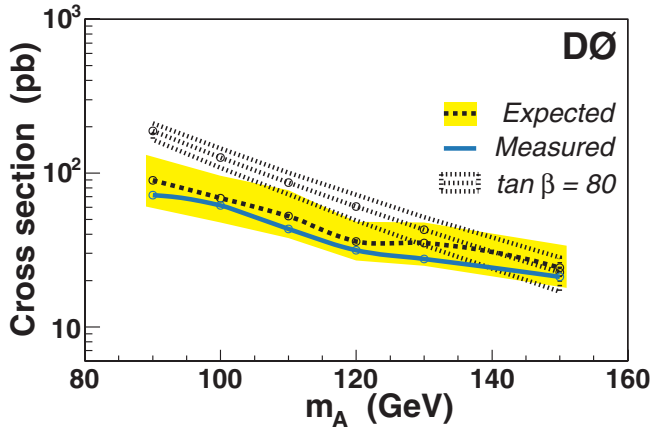


FIG. 4 (color online). The expected and measured 95% C.L. upper limits on the signal cross section as a function of $m_A$. The band indicates the $\pm$1 s.d. range on the expected limit. Also shown is the cross section for the signal at $\tan\beta = 80$ in the "no mixing" scenario of the MSSM, with the theoretical uncertainty indicated by the overlaid band.

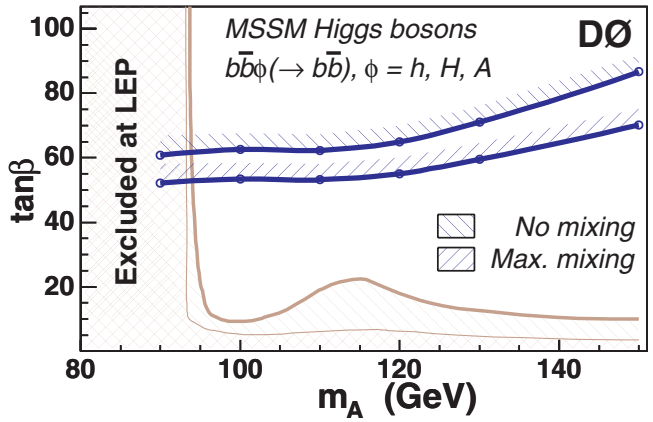


FIG. 5 (color online). The 95% C.L. upper limit on $\tan\beta$ as a function of $m_A$ for two scenarios of the MSSM, "no mixing" and "maximal mixing." Also shown are the limits obtained by the LEP experiments for the same two scenarios of the MSSM [3].

much smaller than from other sources of background uncertainties.

A modified frequentist method is used to set limits on the production of signal [19]. The di-jet invariant mass distributions in triply $b$-tagged events of data, simulated signal, and the normalized background were used as inputs. The value of $\tan\beta$ was varied until the confidence level for signal (C.L.$_S$) was $<5\%$. Figure 3 shows the data, background, and simulated signal at the exclusion limit, for $m_A = 120$ GeV. This is converted to a cross section limit for signal production in Fig. 4, which also shows the expected MSSM Higgs boson production cross section as a function of $m_A$ for $\tan\beta = 80$, and the median expected limit with the background-only hypothesis along with its $\pm 1$ s.d. range. The NLO cross sections and their uncertainties from PDFs and scale dependence are taken from Refs. [5,8]. The MSSM cross section shown in Fig. 4 corresponds to no mixing in the scalar top quark sector [20], or $X_t = 0$, where $X_t = A_t - \mu \cot\beta$, $A_t$ is the trilinear coupling, and the Higgsino mass parameter $\mu = -0.2$ TeV. We also interpret our results in the "maximal mixing" scenario with $X_t = \sqrt{6} M_{\mathrm{SUSY}}$, where $M_{\mathrm{SUSY}}$ is the mass scale of supersymmetric particles, taken to be 1 TeV.

Results for both scenarios of the MSSM are shown in Fig. 5 as limits in the $\tan\beta$ versus $m_A$ plane. The present D0 analysis, based on 260 pb$^{-1}$ of data, excludes a significant portion of the parameter space, down to $\tan\beta = 50$, depending on $m_A$ and the MSSM scenario assumed.

We thank the authors of Refs. [5,8,20] for valuable discussions. We thank the staffs at Fermilab and collaborating institutions, and acknowledge support from the DOE and NSF (USA), CEA and CNRS/IN2P3 (France), FASI, Rosatom and RFBR (Russia), CAPES, CNPq, FAPERJ, FAPESP, and FUNDUNESP (Brazil), DAE and DST (India), Colciencias (Colombia), CONACyT (Mexico), KRF (Korea), CONICET and UBACyT (Argentina), FOM (The Netherlands), PPARC (United Kingdom), MSMT (Czech Republic), CRC Program, CFI, NSERC and WestGrid Project (Canada), BMBF and DFG (Germany), SFI (Ireland), A. P. Sloan Foundation, Research Corporation, Texas Advanced Research Program, Alexander von Humboldt Foundation, and the Marie Curie programs.

*Visitor from University of Zurich, Zurich, Switzerland.

[1] H. P. Nilles, Phys. Rep. **110**, 1 (1984); H. E. Haber and G. L. Kane, Phys. Rep. **117**, 75 (1985).
[2] J. F. Gunion, H. E. Haber, G. L. Kane, and S. Dawson, *The Higgs Hunter's Guide* (Addison-Wesley, Reading, MA, 1990).
[3] The LEP Working Group for Higgs Boson Searches, LHWG, Note No. 2004-01 (unpublished).
[4] T. Affolder *et al.*, (CDF Collaboration), Phys. Rev. Lett. **86**, 4472 (2001).
[5] J. Campbell, R. K. Ellis, F. Maltoni, and S. Willenbrock, Phys. Rev. D **67**, 095002 (2003).
[6] S. Dawson, C. B. Jackson, L. Reina, and D. Wackeroth, Phys. Rev. D **69**, 074027 (2004); S. Dittmaier, M. Krämer, and M. Spira, Phys. Rev. D **70**, 074010 (2004).
[7] J. Campbell *et al.*, hep-ph/0405302.
[8] S. Dawson, C. B. Jackson, L. Reina, and D. Wackeroth, Phys. Rev. Lett. **94**, 031802 (2005).
[9] J. S. Lee *et al.*, Comput. Phys. Commun. **156**, 283 (2004).
[10] M. Carena and H. E. Haber, Prog. Part. Nucl. Phys. **50**, 63 (2003).
[11] E. Boos, A. Djouadi, M. Mühlleitner, and A. Vologdin, Phys. Rev. D **66**, 055004 (2002).
[12] V. Abazov *et al.* (D0 Collaboration) (to be published).
[13] S. Abachi *et al.* (D0 Collaboration), Nucl. Instrum. Methods Phys. Res., Sect. A **338**, 185 (1994).
[14] G. C. Blazey *et al.*, in *Proceedings of the Workshop: "QCD and Weak Boson Physics in Run II"*, edited by U. Baur, R. K. Ellis, and D. Zeppenfeld (Fermilab, Batavia, IL, 2000), p. 47; see Sec. 3.5 for details.
[15] T. Sjöstrand *et al.*, Comput. Phys. Commun. **135**, 238 (2001).
[16] M. L. Mangano *et al.*, J. High Energy Phys. 07 (2003) 001.
[17] J. Campbell, R. K. Ellis, F. Maltoni, and S. Willenbrock, Phys. Rev. D **69**, 074021 (2004).
[18] F. Maltoni and T. Stelzer, J. High Energy Phys. 02 (2003) 027.
[19] T. Junk, Nucl. Instrum. Methods Phys. Res., Sect. A **434**, 435 (1999).
[20] M. Carena, S. Mrenna, and C. E. M. Wagner, Phys. Rev. D **60**, 075010 (1999); **62**, 055008 (2000).